Allman, J.M., R. Jeo, and M.I. Sereno (1994) The functional organization of visual cortex in owl monkeys. In J.F. Baer, R.E. Weller, and I. Kakoma (eds.), *Aotus: the owl monkey*. Academic Press, pp. 287-320.

Aotus: The Owl Monkey

Edited by

Janet F. Baer
California Institute of Technology
Division of Biology
Pasadena, California

Richard E. Weller
Battelle
Pacific Northwest Laboratories
Richland, Washington

Ibulaimu Kakoma
College of Veterinary Medicine
University of Illinois
Urbana, Illinois

This book is printed on acid-free paper.

Academic Press, Inc.
A Division of Harcourt Brace & Company
525 B Street, Suite 1900, San Diego, California 92101-4495

United Kingdom Edition published by
Academic Press Limited
24-28 Oval Road, London NW1 7DX

Library of Congress Cataloging-in-Publication Data

Aotus : the owl monkey / edited by Janet F. Baer, Richard E. Weller, and Ibulaimu Kakoma.
p. cm.
Includes bibliographical references and index.
ISBN 0-12-072405-7
I. Aotus. I. Baer, Janet F. II. Weller, Richard E.
III. Kakoma, Ibulaimu.
QL737.925A94 1994
599.82--dc20 94-7468
CIP

PRINTED IN THE UNITED STATES OF AMERICA
94 95 96 97 98 99 EB 9 8 7 6 5 4 3 2 1

Academic Press
San Diego New York Boston
London Sydney Tokyo Toronto

11

The Functional Organization of Visual Cortex in Owl Monkeys

John Allman and Richard Jeo
Division of Biology
California Institute of Technology
Pasadena, California 91125

Martin Sereno
Department of Cognitive Science
University of California at San Diego
La Jolla, California 92093

I. MULTIPLE MAPS OF THE VISUAL FIELD IN VISUAL CORTEX

The cerebral cortex of the owl monkey is less fissured than that of most higher primates. Because of this feature, Allman and Kaas selected the owl

monkey for their studies of the functional organization of primate visual cortex that began in 1968 (Allman and Kaas, 1971a,b, 1974b, 1975, 1976). These studies led to the discovery of the large expanse of visually responsive cortex that could be subdivided into many visual areas on the basis of receptive field mapping.

An example of the mapping of a cortical visual area is illustrated in Fig. 1. In the experiment, the anesthetized monkey was placed at the center of a translucent plastic hemisphere. The electrical activity of neurons was recorded with microelectrodes in the visual cortex while moving simple visual stimuli on the surface of the plastic hemisphere. The receptive field obtained from each cortical recording site was the area on the hemisphere that when stimulated resulted in an increase in the electrical spiking activity detected by listening to an audio monitor. The receptive fields obtained in this experiment are depicted as broad ovals in the perimeter chart representing the contralateral half of the visual field that is illustrated in the right side of Fig. 1. In this particular experiment the microelectrode was advanced parallel to the medial wall of the occipital lobe, which is illustrated in the lower left part of Fig. 1. Thus, in penetration 1, electrode sites A through D were recorded as the microelecrode advanced and the corresponding visual receptive fields 1A through 1D were mapped. There was a steady progression of receptive fields as the microelectrode was advanced. When the receptive fields for a series of penetrations were plotted, they formed a "map" of the visual field, which is illustrated in the upper left part of Fig. 1. The map is a representation of the contralateral half of the visual field. Figure 1 is the map of the Medial Visual Area, abbreviated as M, which is unique among cortical visual areas because of its relatively large representation of the more peripheral parts of the visual field, which makes it convenient for illustrative purposes. For the other cortical visual areas the mapping principles are the same, but there is a much greater emphasis on the central part of the visual field, which sustains higher acuity.

This investigation has continued for the past 25 years. Sereno, McDonald, and Allman have recently produced the map illustrated in Fig. 2 based on a large number of receptive fields recorded from throughout the visual cortex. The delineation of the inferotemporal areas was based on the anatomical studies of Weller and Kaas (1985, 1987). In Fig. 2, in the upper right-hand corner there is a dorsolateral view of the owl monkey brain with the anatomical location of the areas depicted. The main body of Fig. 2 is an unfolded and flattened version of the owl monkey visual cortex. The star indicates the representation of the center of the visual field, the line of circles indicates the representation of the vertical midline of the visual field, and the line of black squares indicates the representation of the horizontal meridian. The vertical meridian forms the border between the

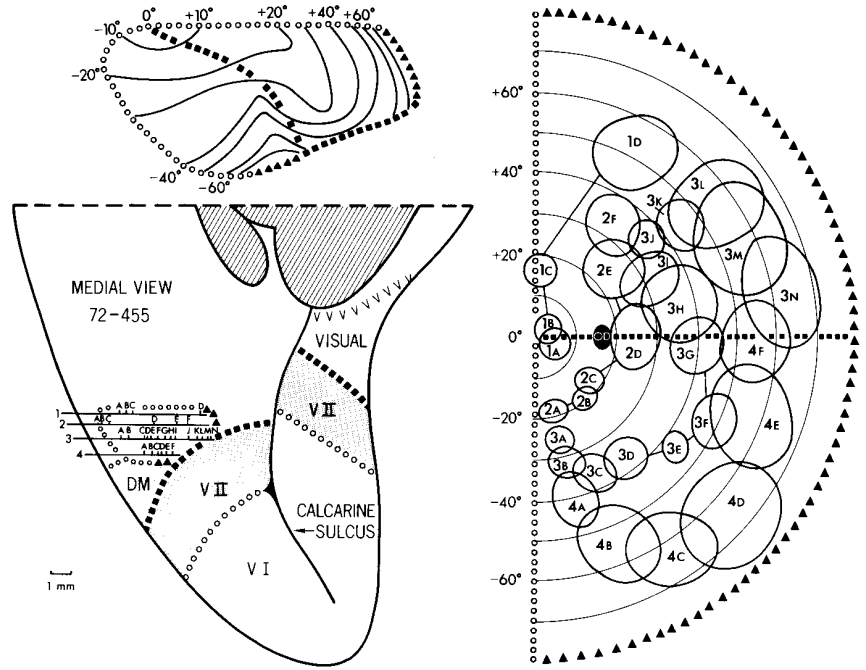

FIGURE 1 Microelectrode recording and receptive field data for the Medial Visual Area in owl monkey 72–455. The diagram on the lower left is a view of the posterior half of the medial wall of cerebral cortex of the left hemisphere with the brain stem and cerebellum removed. Anterior is up and dorsal is to the left in this diagram. Microelectrode penetrations are numbered, and recording sites are indicated by short bars denoted by letters. The corresponding receptive fields are shown in the perimeter chart on the right. In the upper left is an expanded map of the visuotopic organization of the Medial Visual Area. The circles indicate the representation of the vertical meridian (midline) of the visual field; the squares indicate the horizontal meridian of the contralateral half of the visual field; the triangles indicate the temporal periphery of the contralateral hemifield. V I is the First Visual Area, denoted at V1 in the text; V II is the Second Visual Area, denoted as V2 in the text; DM is the Dorsomedial Visual Area; OD indicates the projection of the optic disk or blind spot. Reproduced from Allman and Kaas (1976), with permission from the American Association for the Advancement of Science.

First Visual Area (V1) and the Second Visual Area (V2), and the border between the Ventral Posterior (VP) and Ventral Anterior (VA) Visual areas, as well as many other visual areas. The horizontal meridian forms the border between V2 and a series of adjacent "third tier" visual areas: VP; the Dorsal Lateral Posterior, DLp; the Dorsal Intermediate Area, DI; the Dorsal Medial Area, DM; and finally, area M. The horizontal meridian also forms the border of many other areas.

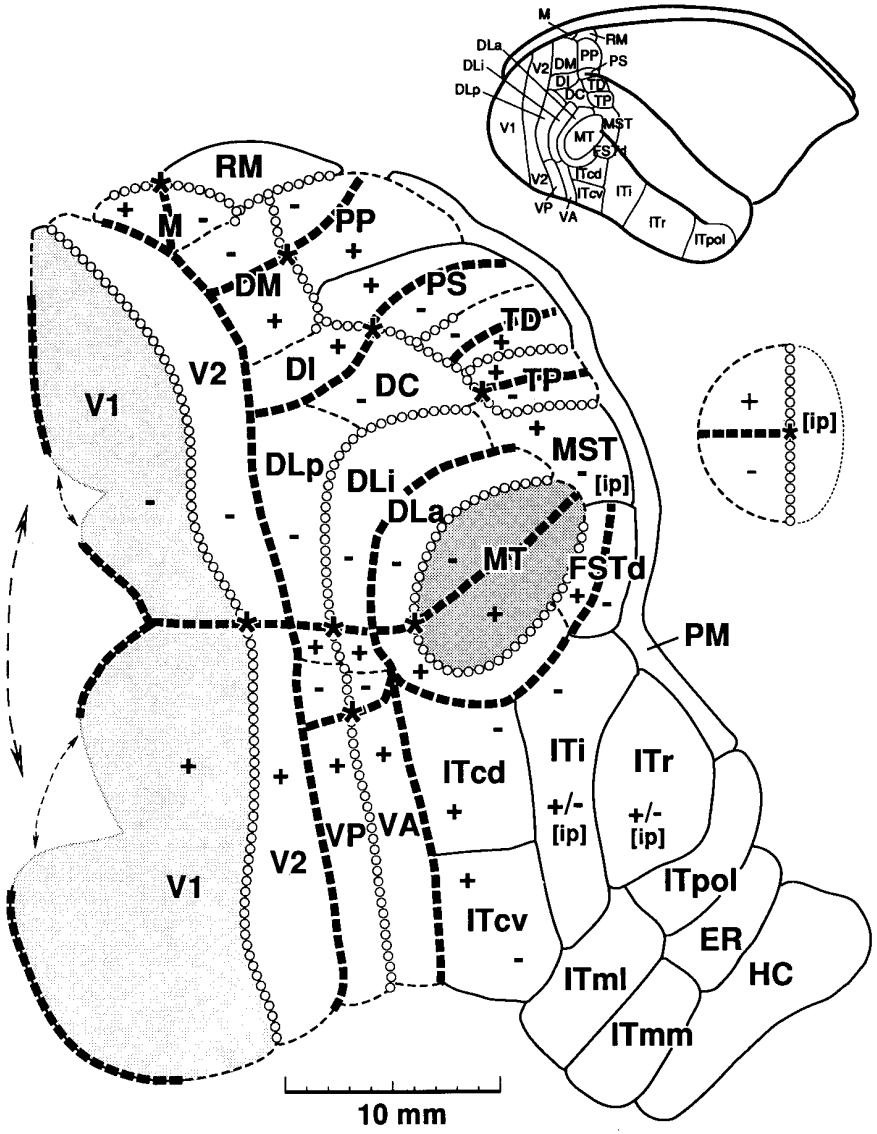

FIGURE 2 Visual cortical areas in the owl monkey (M. Sereno, C. McDonald, and J. Allman, unpublished data). Area boundaries are based on Allman and Kaas (1971a,b, 1974a,b, 1975, 1976), Weller and Kaas (1985, 1987), and Sereno *et al.* (1987; Sereno and Allman, 1991). They were drawn using a cytochrome oxidase-stained flat-mounted hemisphere as a template. A cut was made in V1 in the depths of the calcarine sulcus to allow the cortex to lie flat. Abbreviations: DC, dorsocentral; DI, dorsointermediate; DLa, dorsolateral anterior; DLi, dorsolateral intermediate; DLp, dorsolateral posterior; DM, dorsomedial; ER, entorhinal; FSTd, fundus superior temporal—dorsal division; ITcd, caudal inferotemporal—dorsal division; ITcv, caudal inferotemporal—ventral division; ITi, intermediate inferotemporal; ITml, medial inferotemporal—lateral division; ITmm, medial inferotemporal—medial division; ITpol, polar inferotemporal; ITr, rostral inferotemporal; MT, middle temporal; PM, polymodal; PP, posterior parietal; PS, posterior sylvian; RM, rostromedial; ST, superior temporal; TD, temporodorsal; TP, temporoparietal; VA, ventroanterior; VP, ventroposterior; V1, First Visual Area; V2, Second Visual Area.

II. HISTOLOGICAL FEATURES OF CORTICAL VISUAL AREAS

Figures 3 and 4 are histological sections stained for myelinated fibers through the visual cortex. Figure 3 is a horizontal section from V1 to MT. V1 is characterized by the densely stained stria of Gennari (SG), which is the anatomical basis for the term striate cortex. V2 is characterized by a slightly denser myelin staining in the lower cortical layers. MT is characteristically densely stained for myelin. Figure 4 is a coronal section through MT, which stains out in bold contrast to the adjacent visual areas. The underlying part of V1 in the calcarine sulcus is located below MT.

The corpus callosum connects the two hemispheres and carries the fiber connections that unify the representation of the two halves of the visual field. Figure 5 illustrates the distribution of corpus callosum projections indicated by the dots. Areas V1 and MT are shaded. There is a definite clustering of projections along the border between V1 and V2, and to a lesser extent along the border of MT. The corpus callosum unifies the two halves of the visual field and its termination in these areas approximately corresponds to the representation of the vertical midline of the visual field. This correspondence with the vertical midline also is true for the second discrete band on the ventral surface about 5 mm anterior to striate cortex. Figure 6 illustrates the receptive fields recorded near the vertical midline of the visual field and the callosal band running across the ventral occipital cortex. This band led to the discovery of the twin ventral areas VP and VA.

Figure 7 illustrates a section parallel to the surface of flattened visual cortex stained for the energy-producing enzyme, cytochrome oxidase, from the work of Tootell *et al.* (1985). Area V1 is to the right in this figure and is filled with small dark spots. These are the cytochrome oxidase-rich "puffs," "patches," or "blobs" (Wong-Riley and Carroll, 1984; Horton, 1984; Livingstone and Hubel, 1984). In diurnal monkeys, these cytochrome oxidase-rich spots are clearly related to color processing (Livingstone and Hubel, 1984; Tootell *et al.*, 1988; Ts'o and Gilbert, 1988), but their presence in nocturnal owl monkeys suggests that they have some other, more basic function. Allman and Zucker (1990) have suggested that they are involved in the continuous analysis of luminosity and thus have greater energy requirements than the surrounding lightly stained zones, which are involved in the analysis of statistically rarer events, such as a specific orientation or disparity. Area V2 is characterized by a series of stripes abutting on the V1 border. In the left side of Fig. 7, area MT is an oval of dense

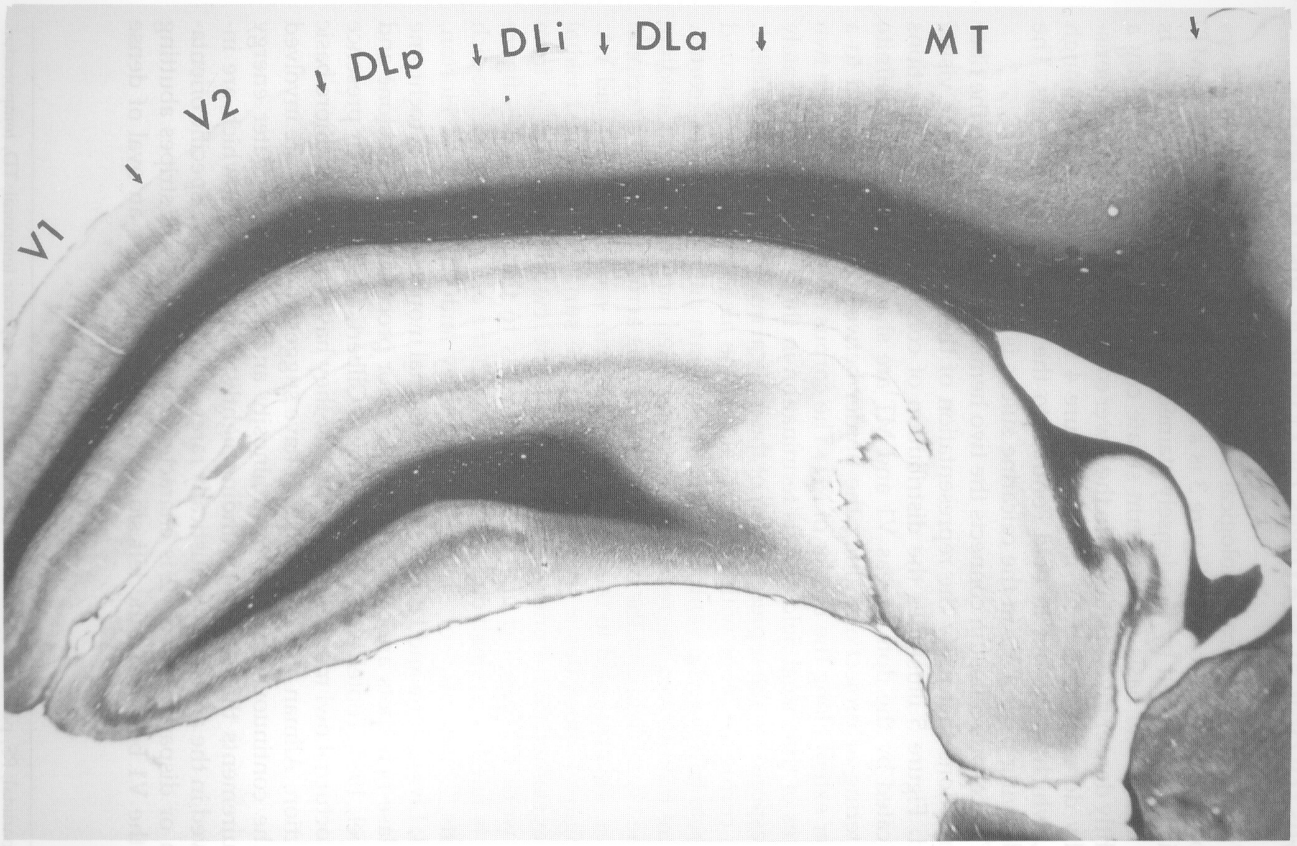

FIGURE 3 An oblique section between horizontal and sagittal through the visual cortex of the owl monkey stained with the Gallyas technique for fibers. Abbreviations are as in Fig. 2.

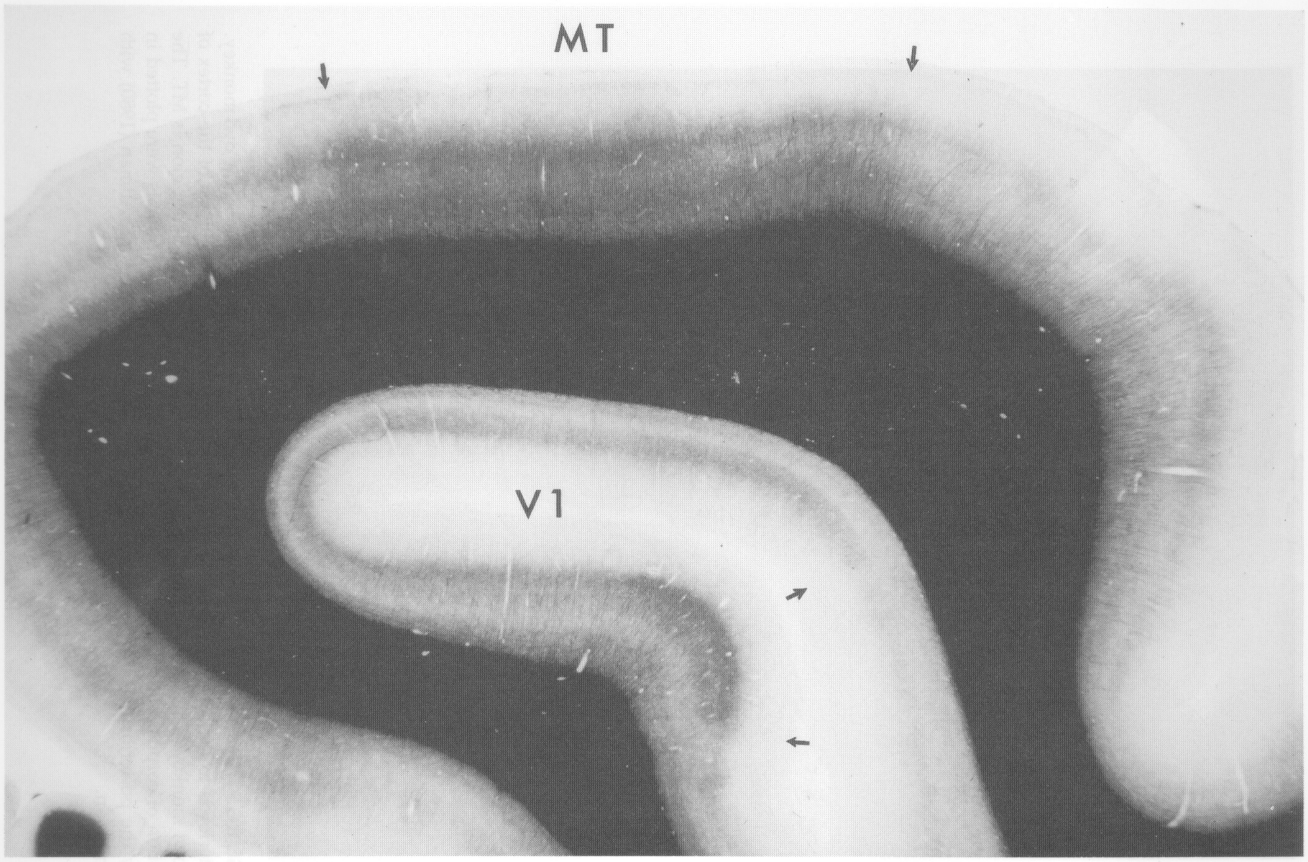

FIGURE 4 A coronal section through area MT and adjacent structure in the owl monkey stained with the Heidenhain technique for fibers.

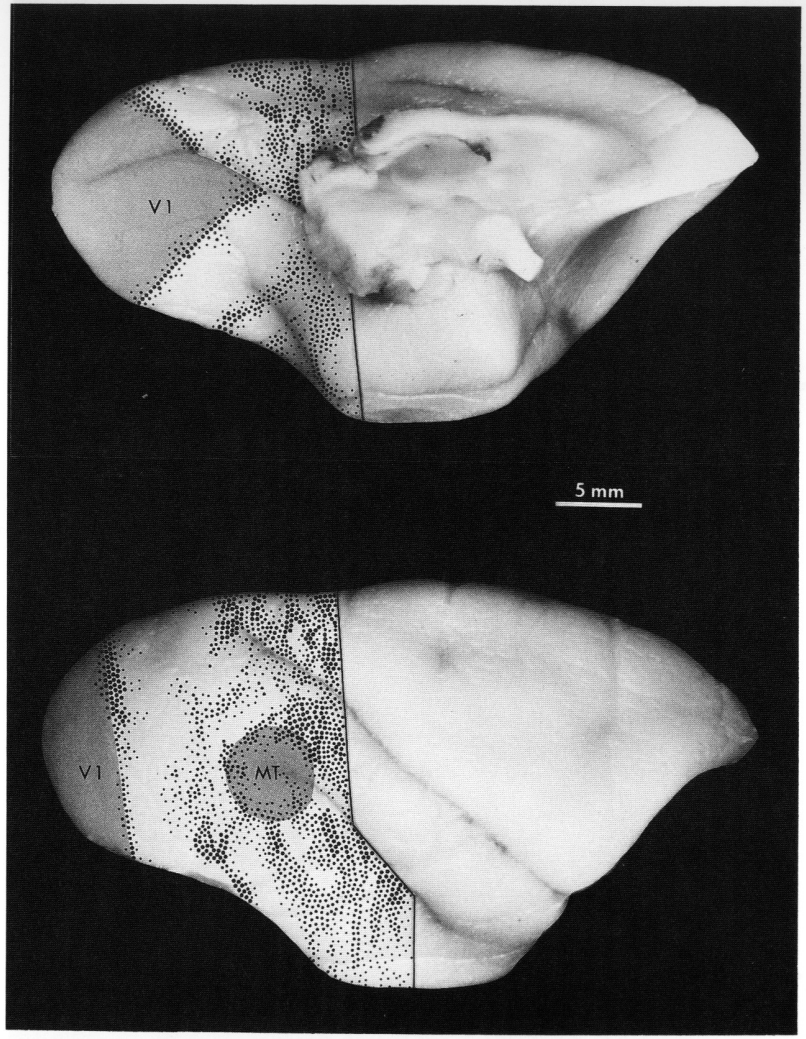

FIGURE 5 Distribution of corpus callosum terminals in the visual cortex of the owl monkey. Posterior is to the left. Dorsolateral (top) and ventromedial (bottom) views of the cortex of an owl monkey. The posterior shaded region is V1 and the oval shaded region is MT. The location of corpus callosum terminals is indicated by the dots; the terminals were plotted in only the posterior half of the cortex. Reproduced from Newsome and Allman (1980) with permission.

cytochrome oxidase staining, which is probably related to the high energetic requirements inherent in processing temporarlly varying stimuli (see the following). Within the densely stained oval are islands of lower activity. The work of Born and Tootell (1992) suggests that the antagonistic surround mechanisms described in the next section are stronger in the lightly stained zones within MT.

III. NEURAL RESPONSES IN THE CORTICAL VISUAL AREAS

A. Overview

Figure 8 summarizes some of the other important response properties of neurons in these areas. In each case the size of the square indicates the relative strength of the response property as expressed in the area. Neurons in area DL are significantly less orientation selective than in MT, DM, or M, but DL neurons are much more dimensionally selective (i.e., sensitive to stimulus shape). Area MT neurons are more sensitive to direction of motion than DL neurons, which in turn are more sensitive to directionality than neurons in DM or M. Neurons in MT are much more sensitive to the motion of fields of random dots than are neurons in other areas. Area DL contains the greatest emphasis on the representation of the central visual field, whereas area M has the least emphasis on central vision.

B. Responses to Flashed and Moving Stimuli

Figure 9 illustrates the summed histogram responses of populations of neurons recorded from areas MT, DL, M, and DM, when an optimally oriented stationary bar of light was presented. (This work was done before Sereno, McDonald, and Allman discovered the subdivisions of Dl.) The histograms for area MT have an initial response latency of 33 msec with a strong transient peak response at 59 msec, followed by a trough at about 175 msec and then a modest rebound in activity. Area M has a similar histogram with a slightly slower initial response at 42 msec. Area DL has a much slower initial response at 63 msec, a peak at 84 msec, and a much larger tonic level of activity. Area DM is intermediate between DL and M both anatomically and in its histogram. These data indicate that areas MT and M have mainly a fast, transient response to visual stimuli, whereas area DL has a much slower and more sustained response. These response histograms reflect a fundamental difference between areas MT and M, which are involved in the analysis of motion, and area DL, which is more involved in the analysis of stimulus form.

Figure 10 illustrates histograms of the directionality of neurons in these four areas. The higher the index, the greater the differential sensitivity of

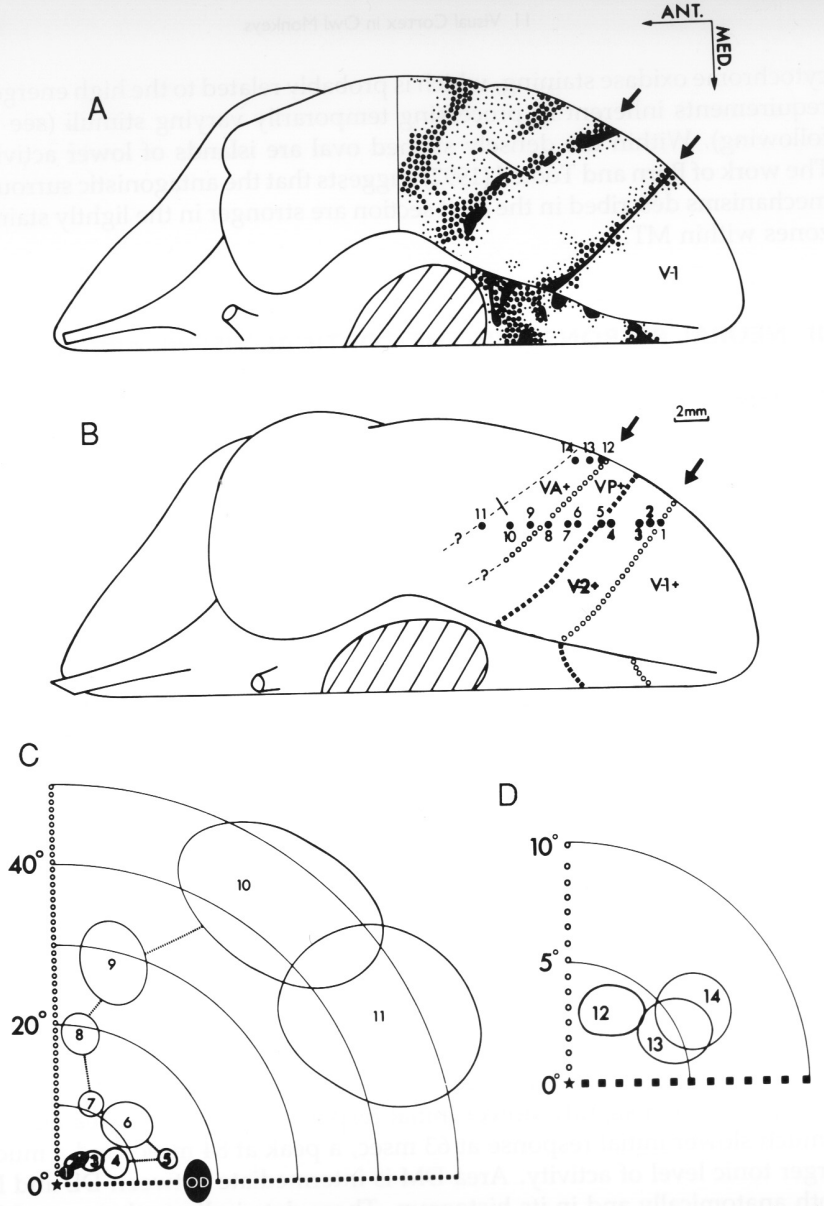

FIGURE 6 Comparison of anatomical results with physiological data for the ventral surface of owl monkey visual cortex. (A) The pattern of degeneration on the ventral surface of owl monkey 78-3. Heavy degeneration is solid black, moderate degeneration is represented by large dots, and light degeneration by the small dots. (B) Electrophysiological recording sites (1 through 14) on the ventral surface of owl monkey 72-343. The location of the recording sites is based on a histological reconstruction of the electrode tracks superimposed on a photograph of the ventral surface taken postmortem. Open circles denote the vertical meridian representations and the solid squares signify the horizontal meridian representation. Dashed lines represent uncertain boundaries. (C) Receptive fields for recording sites 1 through 11. The black receptive field is in V1, the gray-shaded receptive fields are in V2, and the unshaded receptive fields are in VP and VA. Note the progression of receptive fields from the hortizontal meridian (recording site 5) at the V2–VP border to the vertical meridian (recording site 8) at the VP–VA border. (D) Receptive fields for recording sites 12–14. Note the change in scale between C and D. Recording site 12, near the VP–VA boundary, yielded a receptive field very near the vertical meridian. The physiological representations of the vertical meridian illustrated in B appear remarkably similar to the distinct bands of callosal degeneration in A (solid arrow). The data of C and D also illustrate the progression from the representation of the center-of-gaze laterally to the representation of the periphery medially. Abbreviations as in Fig. 2. Reproduced from Newsome and Allman (1980) with permission.

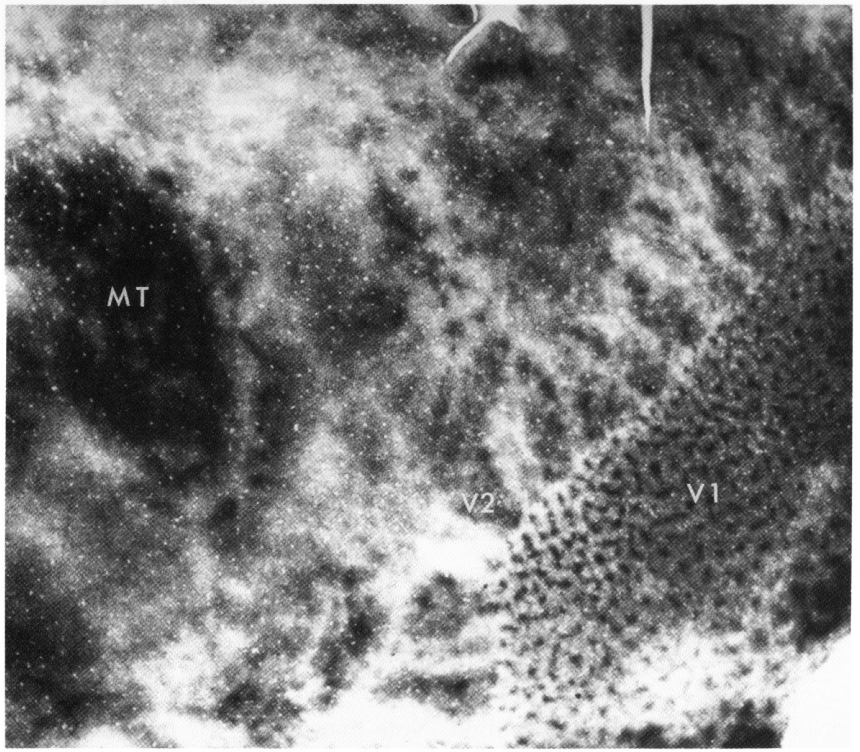

FIGURE 7 Portion of a flattened piece of visual cortex from an owl monkey, sectioned parallel to the surface and stained for cytochrome oxidase activity. Posterior is to the right; dorsal is up. The posterior region containing the fairly regular array of dark spots is V1; the adjacent narrow region containing transverse stripes is V2. The dark-stained oval to the left is MT. Reproduced from Tootell *et al.* (1985) with permission.

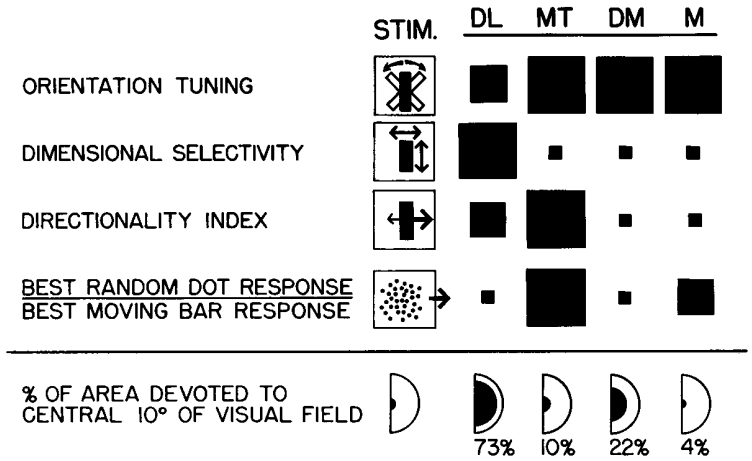

FIGURE 8 Functional specializations in the extrastriate cortical visual areas of the owl monkey based on Baker *et al.* (1981) and Petersen *et al.* (1980). The functional attributes are listed on the left; a pictoral representation of the functional attribute is illustrated in the leftmost column. The four columns labeled DL, MT, DM, and M indicate the relative strength of the functional attribute in that area by the magnitude of the square. The relative representation of the central 10 degrees of the visual field is indicated in the horizontal column in the bottom of the figure.

the neurons to direction of motion. Note than in MT the neurons cluster around a directionality index of 0.9 to 1.0, indicating that they are very sensitive to direction of motion.

Figure 11 illustrates the responses recorded sequentially from a series of 12 neurons in a single vertical penetration perpendicular to the surface of MT. On the left are responses to different directions of bar motion; on the right are responses to flashed bars of different orientations. Note that the first 11 neurons responded optimally to the horizontally oriented flashed bar and that the 12th neuron was inhibited by horizontally oriented flashed bars. The microelectrode was passing down a cortical column defined by preference for horizontal bar stimuli. It is interesting to note that the first 6 neurons in this penetration preferred a horizontal bar moving downward, and that then there was an abrupt shift to horizontal bars moving upward until the last neuron, in which the preferred stimulus was a vertical bar moving to the left. These data suggest that the basic columnar system in MT is for orientation and that grafted upon this is a second system for direction of motion. From the data presented in Fig. 11 it is also possible to interpret the directional preference to be related to cortical lamination, however, there is no other evidence to support the notion of laminar specialization for direction.

C. Effects of Motion Adaptation in Area MT

The presence of adjacent neuron populations specialized for detecting opposite directions of motion suggests a possible mechanism for the "waterfall illusion" or "motion aftereffect." When an observer gazes steadily at an array of stimuli moving in a particular direction for a few minutes, and then the stimulus movement stops, the observer will see the stationary array appear to move in the opposite direction. Thus motion perception may be the product of the precise balance between oppositely tuned populations of neurons. Figure 12 illustrates the influence of adapting motion with random dot backgrounds on the responses of MT neurons. The top two histograms in Fig. 12B were the responses to bar motion in the opposite and preferred direction of motion when the random dot background was stationary. When the background random dots moved in the opposite to the preferred direction of the cell for 20 sec before being tested with a bar moving in the preferred direction, there was a substantial enhancement of the response. When the background random dots moved in the preferred direction of the cell prior to testing with bar moving in the preferred direction, the response was substantially reduced. When the two effects are combined, directionally selective neurons show a large effect from prior motion adaptation.

D. Responses from beyond the Classical Receptive Field

The true receptive fields for MT neurons are very much larger than the classical receptive fields mapped against a stationary background. The stimuli presented in the nonclassical field strongly and selectively influence the responses to stimuli presented within the classical receptive field. For example, in the left half of Fig. 13, the classical receptive field was the small central square containing moving dots. The directional tuning curve below this shows the responses elicited by different directions of movement of random dot array. The optimal direction of motion was horizontal to the right (zero degrees). When this central square was stimulated with random dots moving in the optimal direction and simultaneously the surrounding field was stimulated with moving dots, there was substantial suppression of the response by background movement in the direction that was optimal for the center, and there was considerable enhancement of the response by background movements in the direction opposite to the optimal direction. It should be noted that no observable response could be obtained from this neuron by stimulating the surround by itself. Thus the response from the classical receptive field was contingent on what was happening elsewhere in the visual field in a directionally antagonistic way. This is probably an important mechanism for the integration of local and global motion in visual

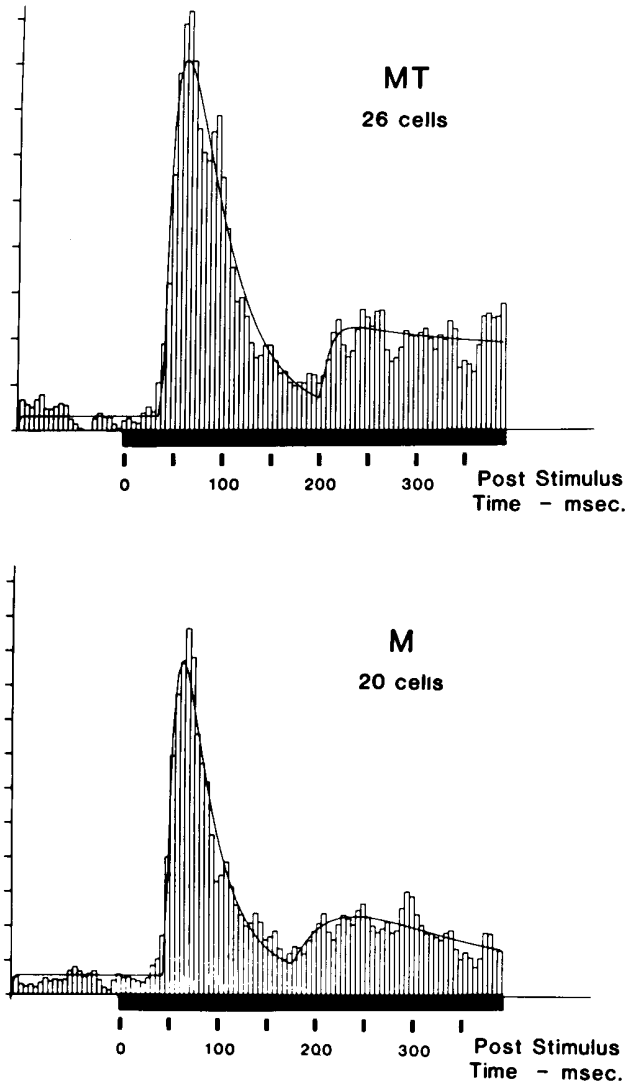

FIGURE 9 Panels display the averaged peristimulus histogram for the response to an optimally oriented flashed bar in the four visual areas sampled. The histogram bins are 5 msec wide. Time since stimulus onset is represented on the horizontal axis with responses before 0 msec being spontaneous activity. The vertical axis was normalized to the peak response for each panel. Superimposed on each histogram is the best-fitting curve obtained by using a random search algorithm. Reproduced from Petersen *et al.* (1988) with permission.

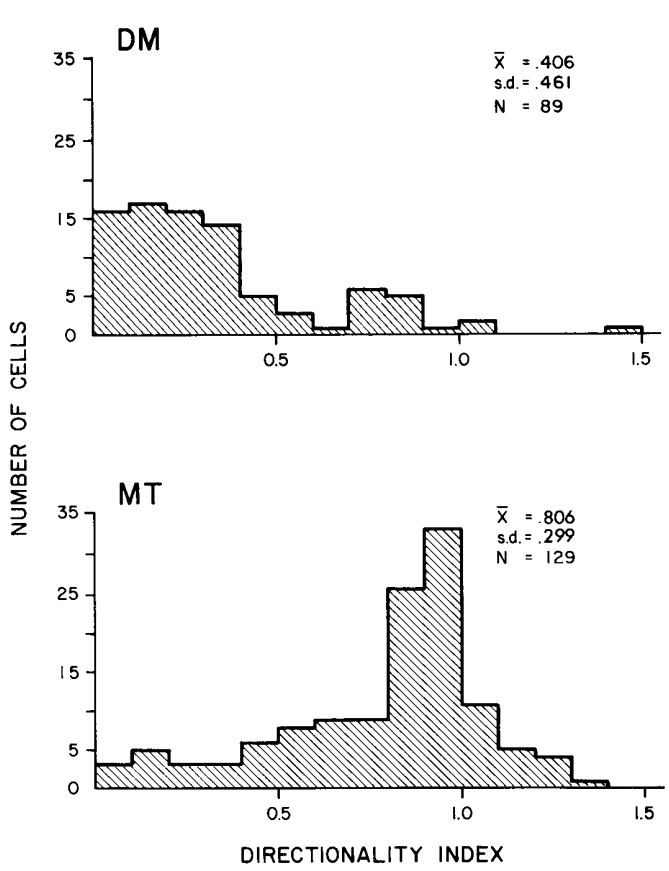

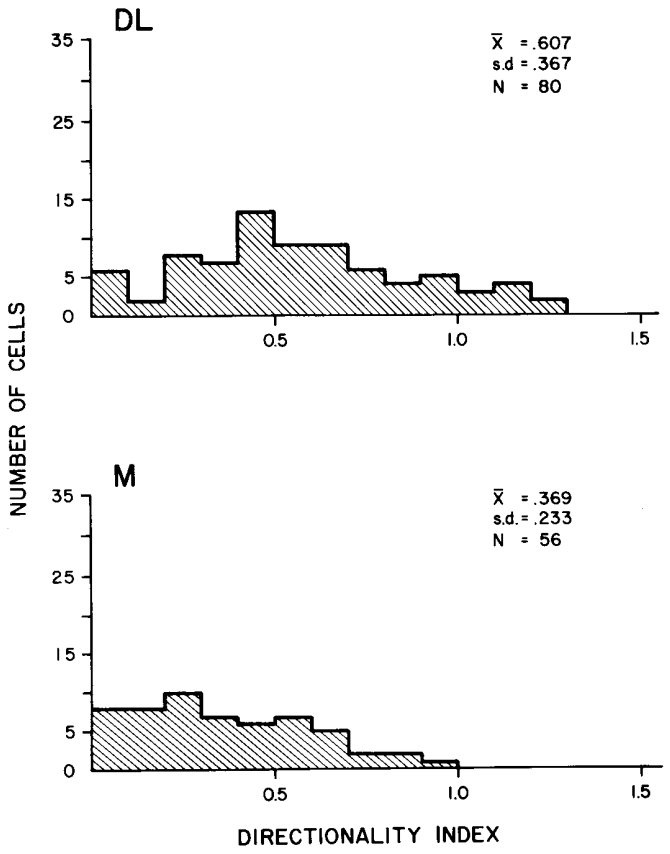

FIGURE 10 Distribution of directionality indices for neurons recorded from DM, DL, MT, and M. The directionality index was (1 minus opposite direction response divided by the best direction response). Reproduced from Baker *et al.* (1981) with permission.

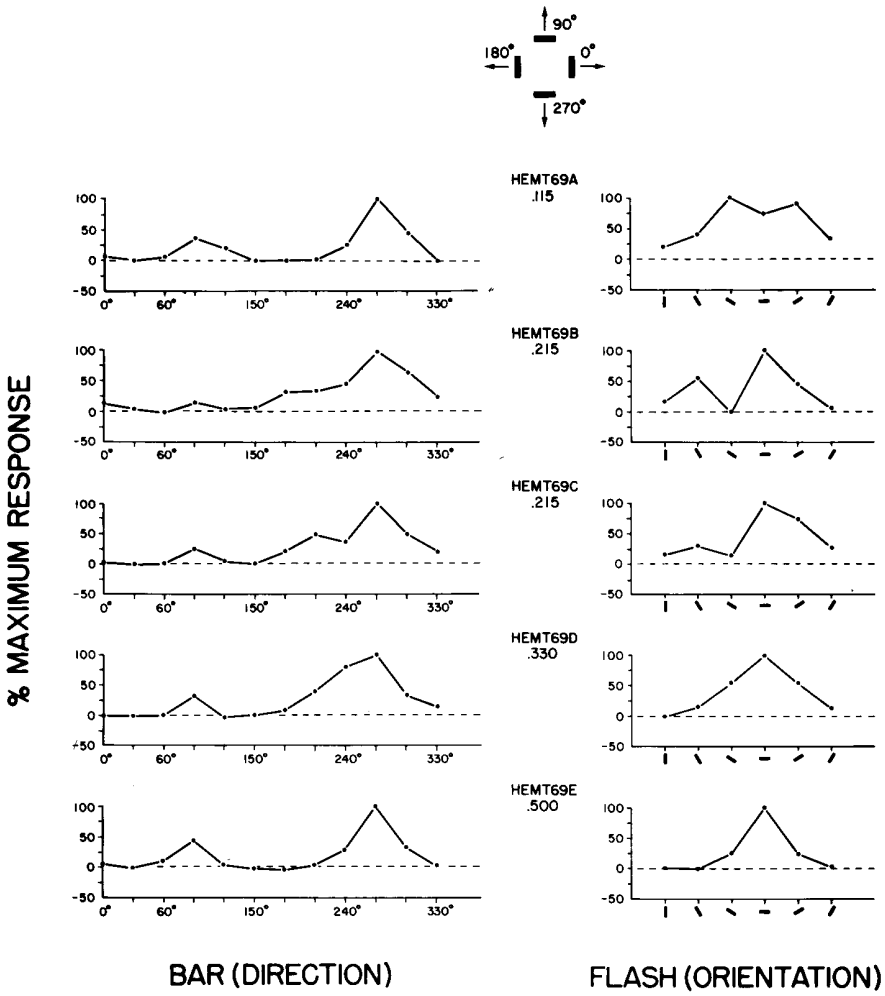

FIGURE 11 Direction and orientation selectivity for a series of neurons recorded in a single penetration nearly perpendicular to the surface of MT. A pair of graphs is illustrated for each unit (HEMT69A through L). The depth beneath the surface at which each cell was recorded is given beneath each identifying number. An electrolytic lesion was made at the bottom of the microelectrode track. Cells A through J were located in layers II and III: cells K and L were located in layer IV. Graphs on the left illustrate the average response of each cell to five presentations of a 20 × 1 degree light bar at 12 different angles. HEMT69A through F preferred 270 degrees; HEMT69G through K preferred 90 degrees. Graphs on the right illustrate the average response of the cells to 10 presentations of a flashed bar at the orientations shown. All cells except the last preferred the horizontal orientation; the last was inhibited by horizontal bars. The direction of movement was 90 degrees to the bar orientation, thus the preferred directions 270 degrees (down) and 90 degrees (up) are consistent with the preferred horizontal orientation. Reproduced from Baker *et al.* (1981) with permission.

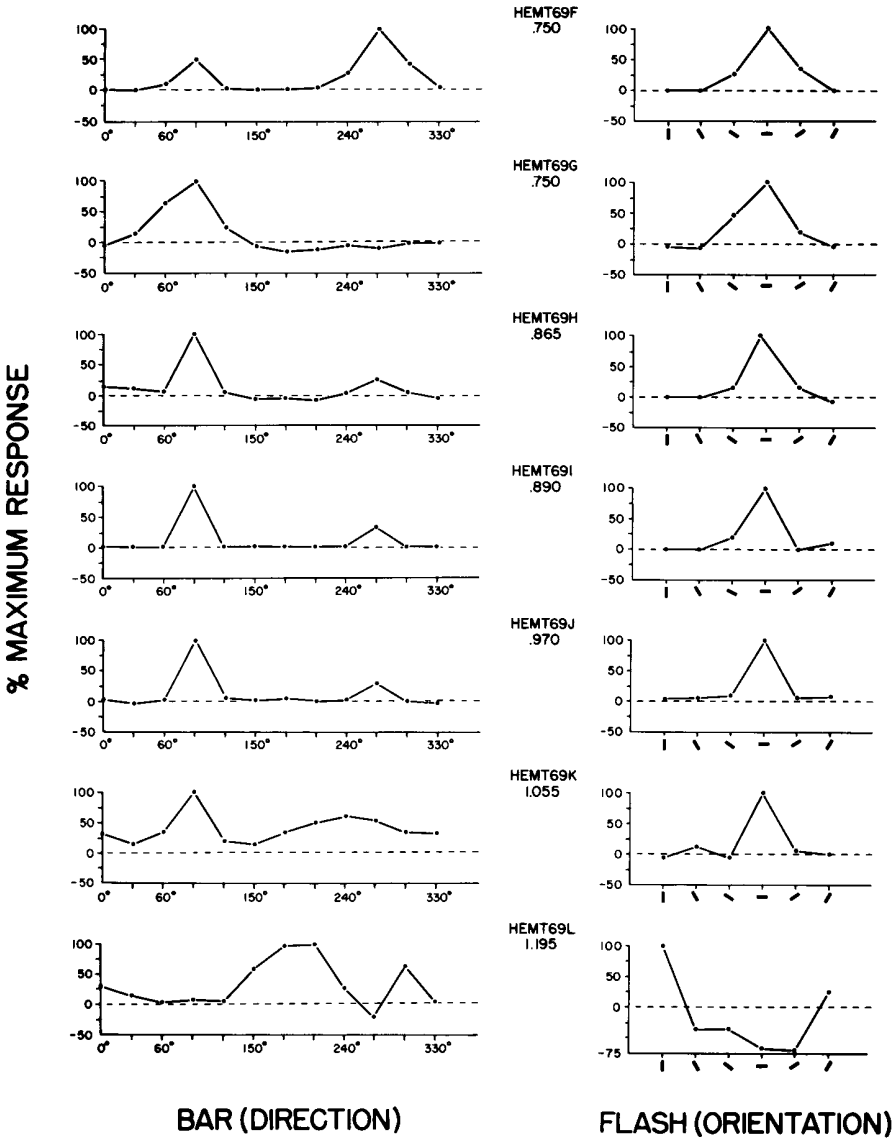

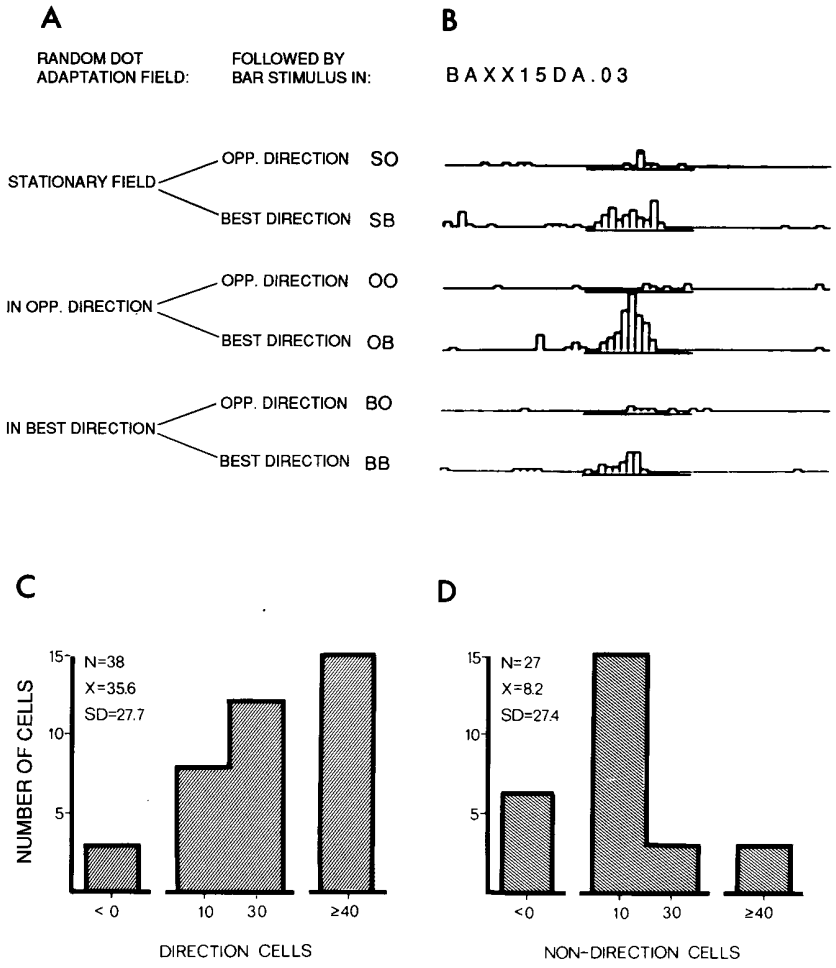

FIGURE 12 (A) Diagrammatic representation of an adaptation series. A 20-sec period of adaptation to stationary noise or noise moving in either the best or opposite directions was followed by a bar stimulus moving in the best direction or opposite direction. These six conditions were pseudorandomly interleaved and presented five times each. (B) An example of an adaptation series. Note that the response is strongest after adaptation in the opposite direction, and weakest after adaptation in the best direction. (C, D) The distribution of adaptation indices for directional and nondirectional cells. The AI was calculated by adding the enhancement after adaptation in the opposite direction to the suppression after adaptation in the best direction. The AI's for directional cells are generally high, whereas those for the nondirectional cells tend to congregate near zero. The difference between these distributions is statistically significant at the 0.001 level. Reproduced from Petersen *et al.* (1985) with permission.

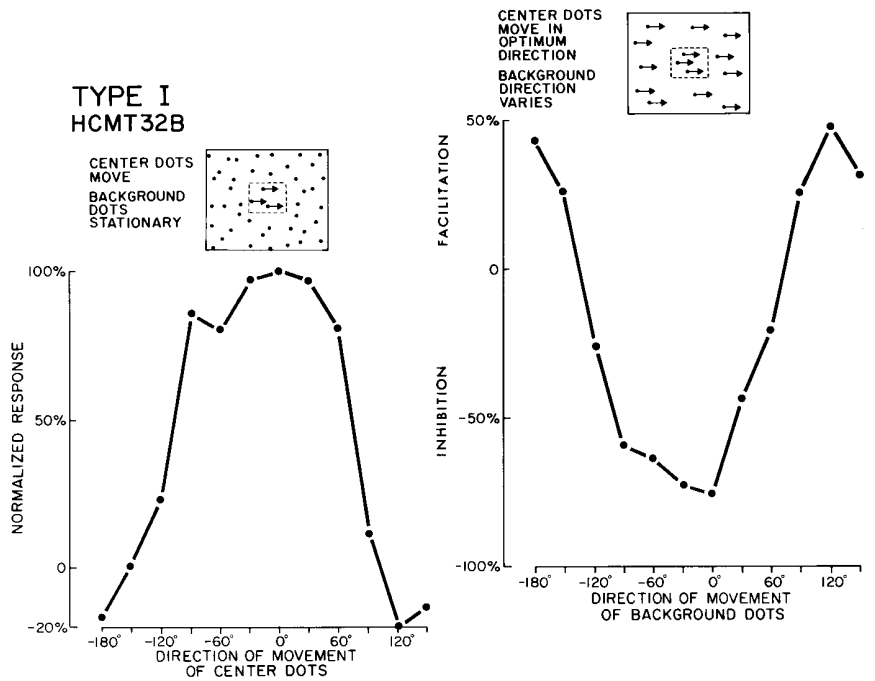

FIGURE 13 Direction-selective neuron with an antagonistic direction-selective surround recorded from area MT in an owl monkey. The left graph depicts the response of the cell to 12 directions of movement in an array of random dots within an area coextensive with its CRF. The response is normalized so that 0% is equal to the average level of spontaneous activity sampled for 2-sec periods before each presentation. Negative percentages in the left graph indicate inhibition relative to the level of spontaneous activity. In the left graph, the response to the optimum direction is 100%. The right graph depicts the response of the cell to different directions of background movement while the classical receptive field was stimulated by the array moving in the optimum direction during the 2-sec sample periods preceding background movement, and thus a response of -100% in the left graph is equivalent to 0% in the right graph. The stimulus conditions are depicted schematically above each graph. In the experiment, the dots were 50% dark and 50% light and the background was much larger relative to the center than is depicted schematically. Reproduced from Allman *et al.* (1985) with permission of Annual Reviews.

perception. This type of neuron constituted 44% of the MT population; 30% were suppressed equally by all directions of background movement; another 18% had more complex surround responses; and only 8% lacked a response from the surround.

Figure 14 is the combined histogram for 42 MT neurons that showed surround responses. In the lower histogram there were continuously moving random dots presented in the classical receptive field and background

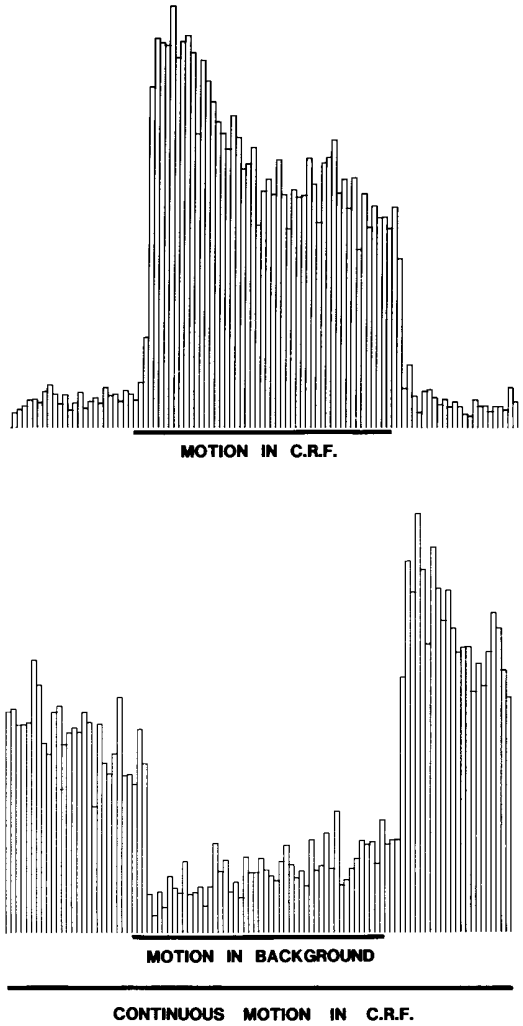

FIGURE 14 The top histogram illustrates the combined responses of 42 MT neurons to random dots moving for a 2-sec period in the preferred direction within their classical receptive fields, with the background stationary. In the lower histogram, the same MT neurons were stimulated continuously with random dots moving in the preferred direction within their classical receptive fields and then tested for a 2-sec period in which the random dots in the surrounding regions also moved in the same direction. Each bin represents 40 msec. The histograms were constructed by normalizing with the largest 40-msec bin in the histogram for each cell and then combining the histograms. Reproduced from Allman *et al.* (1985) with permission of Annual Reviews.

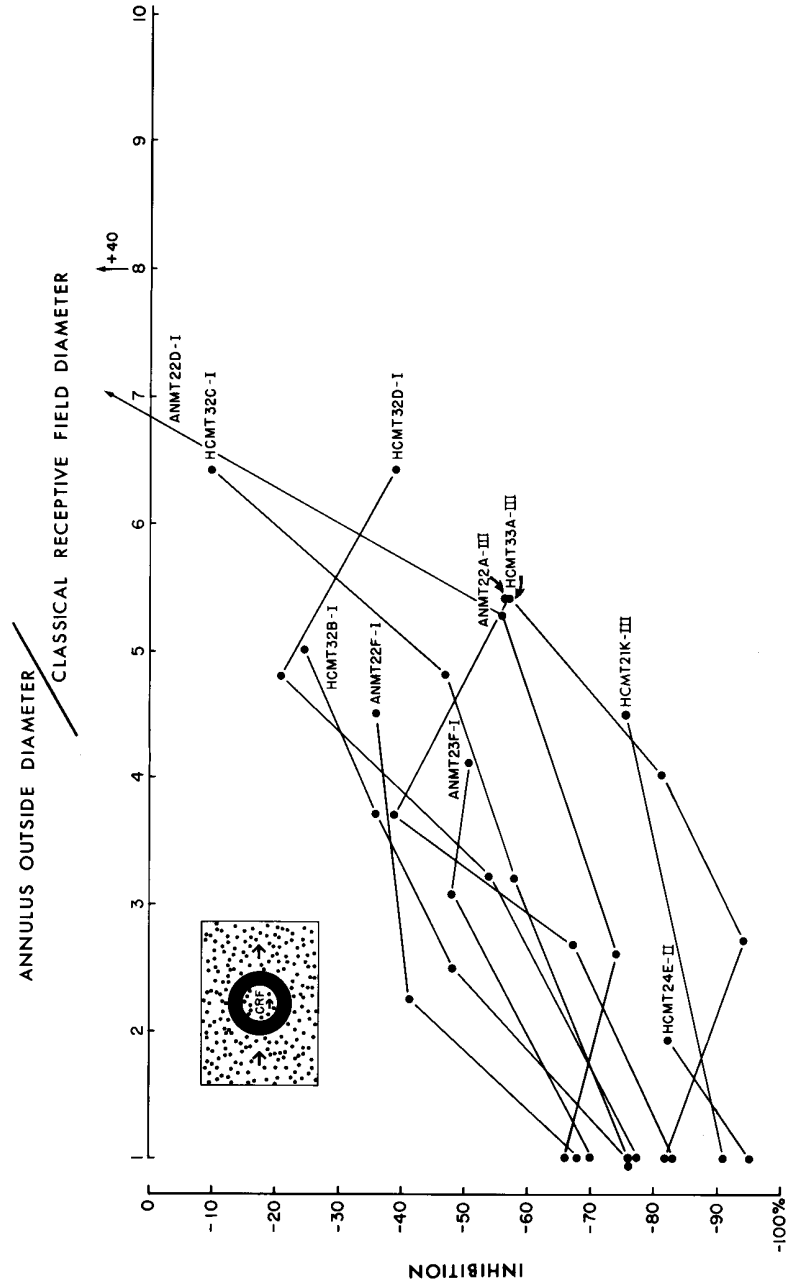

FIGURE 15 The effect of varying the outside diameter of masking annuli of the surround on the response from the classical receptive field in 10 neurons recorded from area MT in the owl monkey. The stimulus conditions are depicted schematically, but in the experiments the dots were 50% dark and 50% light and the surround was much larger. The dots in the center and the surround moved in the optimum direction for the classical receptive field. The inside diameter of the masking annulus corresponds approximately to the diameter of the classical receptive field. The abscissa corresponds to the ratio of the outside diameter of the masking annulus to the diameter of the classical receptive field. Reproduced from Allman *et al.* (1985) with permission of Annual Reviews.

motion in the same direction was presented for 2 sec. There was immediate strong suppression due to the surround stimulation followed by a strong rebound in activity following cessation of the surround movement.

Figure 15 illustrates the extent of the surround in 10 MT neurons. An annulus of varying diameter was used to mask parts of the surround. The annuli had to be very large, more than 7 times the diameter of the classical receptive field, in order to block the surround inhibition. Thus the area of the true receptive field for MT neurons is on the order of 50 times greater than that of the classical receptive field.

The antagonistic organization of MT neurons extends to the velocity of motion. Figure 16 illustrates a velocity tuning curve for a MT neuron with an optimal velocity of 16 degrees per second. When this neuron was stimulated with a bar sweeping at 16 degrees per second and simultaneously the velocity of background motion was varied, there was maximal suppression of background motion at 16 degrees per second. This effect was even more pronounced in V1 and V2 (Fig. 17). Receptive fields with this antagonistic velocity processing were predicted in a theoretical paper by Nakayama and Loomis (1974) as a possible neural basis for kineopsis, or depth perception through the analysis of the differential motion.

E. Sensitivity to Stimulus Shape in Area DL

The responses of DL neurons stand in marked contrast to those of MT. They are slower and more sustained, and can give continuous responses to stationary stimuli. DL neurons are very sensitive to the shape of stimuli, irrespective of their exact location within their classical receptive fields. Figure 18 illustrates the dimensionally selective properties of DL neurons in contrast to responses obtained from other areas. For example, in the upper left graph in Fig. 18, the responses of a DL and a DM neuron are shown for stimuli of different length. The DM neuron's response reached a plateau but did not diminish with increasing bar length; the DL neuron's response after reaching a maximum decreased with increasing bar length. When the best bar length for each DL neuron was compared with the classical receptive field length in the same dimension, it was clear that many DL neurons preferred lengths that were much shorter than the length of the classical receptive field. This was not the case for neurons in MT, DM, and M. Similar results were obtained for bar width and spot diameter. Figure 19 illustrates the preferred shapes observed in DL neurons.

F. Stereopsis

Stereopsis has been relatively little studied in the owl monkey. However, Fig. 20 illustrates data that indicate that tuned excitatory and near-far cells exist in the owl monkey as has been reported in macaque monkeys (Poggio

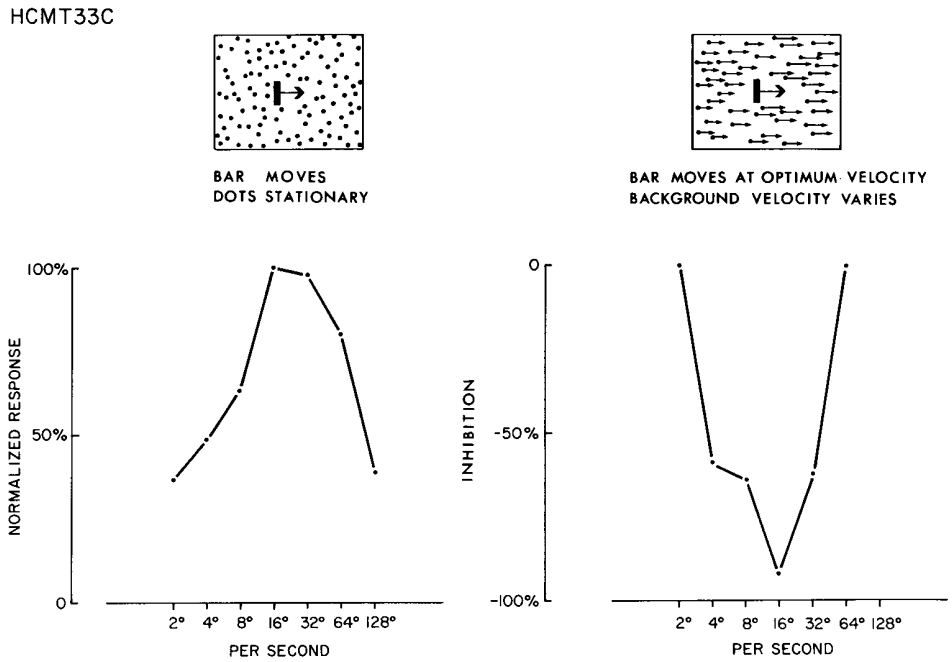

FIGURE 16 The effect of center and background velocity on a neuron recorded from area MT in the owl monkey. The left graph is a velocity-tuning curve for a bar moving in the preferred direction with the background stationary. The right graph is a velocity-tuning curve for background movement while simultaneously presenting the bar moving at the optimum velocity (16 degrees per second). In the background velocity experiments, the background dots stimulated both the classical receptive field and the surround; however, in these experiments, covering the surround eliminated the inhibitory effect. Reproduced from Allman *et al.* (1985) with permission of Annual Reviews.

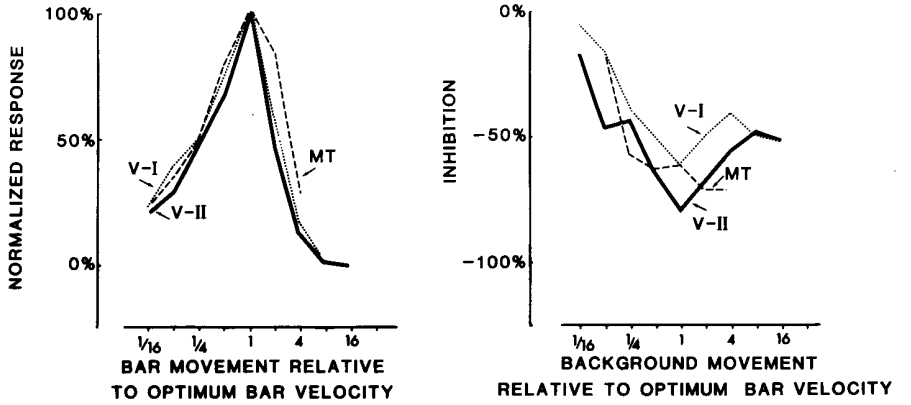

FIGURE 17 Median response curves for bar and background velocity experiments in V1, V2, and MT. Reproduced from Allman *et al.* (1990) with permission.

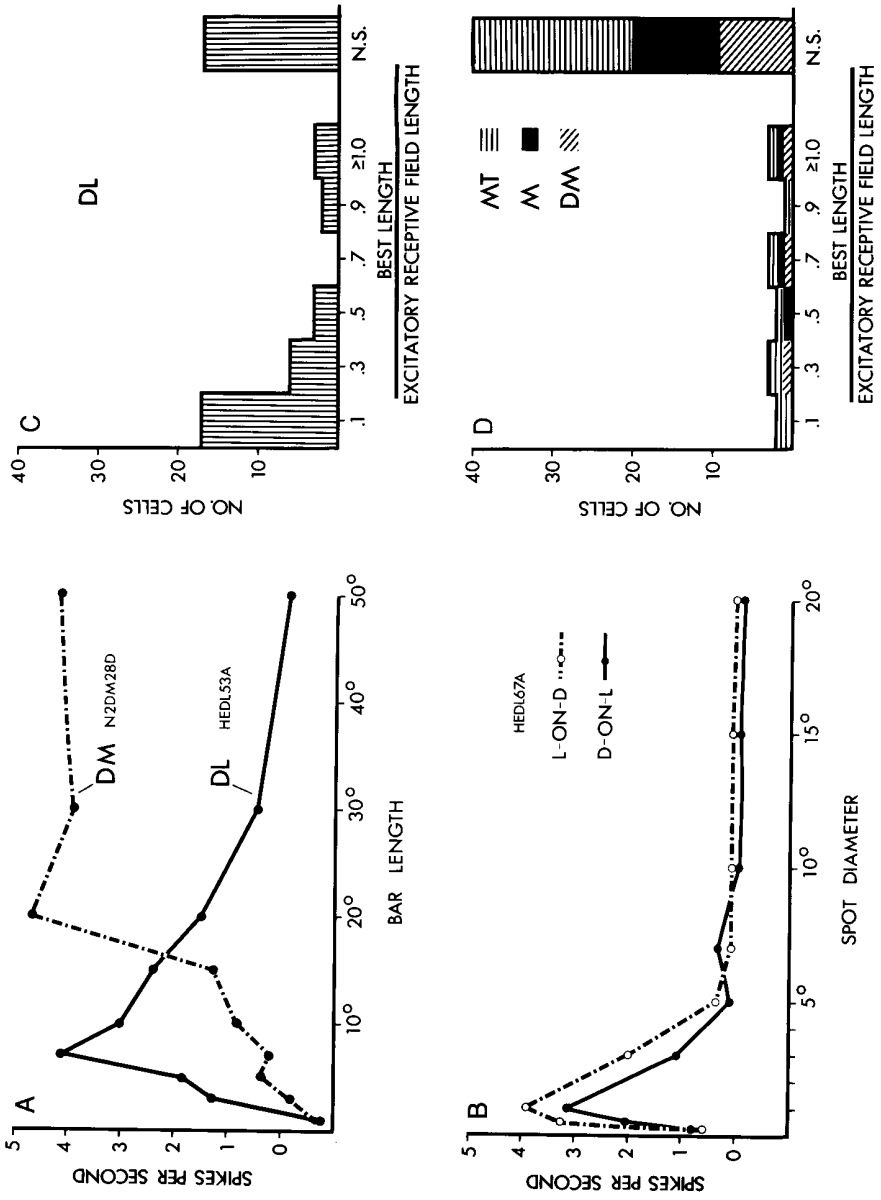

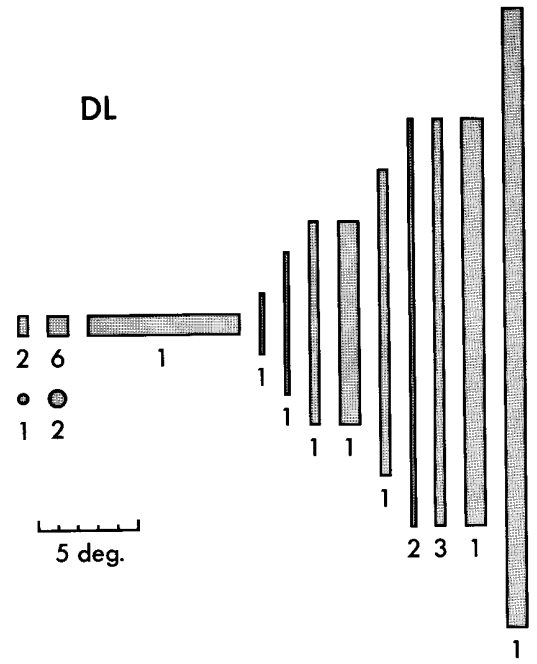

FIGURE 19 Optimal stimulus dimensions for cells recorded from area DL in the owl monkey. From S. E. Petersen, J. F. Baker, and J. M. Allman, unpublished data.

and Fischer, 1977). We trained an owl monkey to report the orientation of dynamic random dot stereograms (J. Allman and F. Miezin, unpublished data) and thus we believe that owl monkeys see in stereoscopic depth.

IV. THE BEHAVING OWL MONKEY PREPARATION

The owl monkeys offers important advantages for use in the study of visual cortex function in the behaving animal. The cortical areas have been

FIGURE 18 (A) Responses of two units to different bar lengths. Each data point is the average of five stimuli presented in pseudorandom order. HEDL53A (solid line) was recorded from DL and shows marked selectivity. N2DM28D (dashed line) illustrates the typical response profile for cells outside of DL, in which the cell summates up to a certain value, whereupon the response levels off. The length of the classical receptive fields for both cells was 20 degrees. (B) Responses of a DL neuron to light (open circles) and dark (solid circles) spots of different diameters. (C, D) Optimal bar length is expressed as a percentage of the comparable dimension of the classical receptive fields. Cells with a length selectivity index of less than 0.5 were considered to be nonselective and are represented by bins at the right. Reproduced from Petersen *et al.* (1980) with permission.

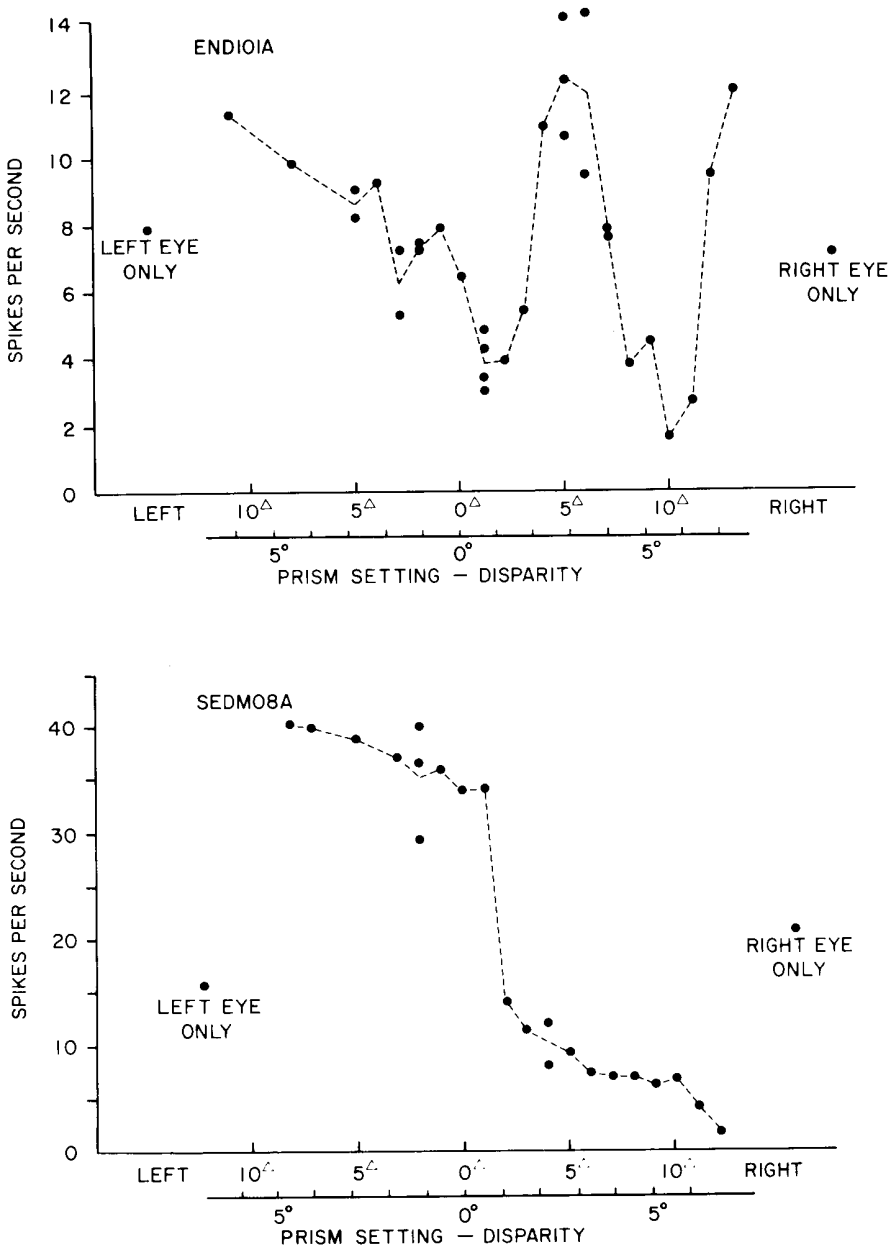

FIGURE 20 An example of a tuned excitatory binocular disparity neuron recorded from area DI (upper graph) and a near-far disparity neuron recorded from area DM (lower graph) in the owl monkey. The disparity values are not corrected for eye position. From J. M. Allman, S. E. Petersen, and J. F. Baker, unpublished data.

extensively mapped and many are located on the smooth dorsolateral surface of the brain. Thus it is relatively easy to position recording electrodes in the desired cortical location. This would also facilitate the injection of agents to block temporarily any neural activity, such as muscimol, during recording and perceptual experiments. The large array of cortical visual areas on the smooth dorsolateral surface would also greatly facilitate optical recording experiments.

We have developed new training procedures and built equipment specially adapted for owl monkey training and electrophysiology, because owl monkeys do not respond well to standard procedures used for training macaque monkeys. Owl monkeys, and all other New World monkeys, cannot sit comfortably in training chairs designed for macaque monkeys because they lack ischial callosities. We designed a special training apparatus consisting of a lexan alcove with two keys, which attaches to the cage in which the monkey lives. This alcove is designed to fit the owl monkey's natural squatting position. The monkey learns to enter the alcove and report discrimination of various images by pressing one of the two keys for a fruit juice reward. We monitor fluid intake to ensure that the monkey receives adequate amounts, and free water is offered for several hours after each training session. Owl monkeys also require much more gentle habituation to restraint than do macaque monkeys. To perform microelectrode or optical recording while the monkey performs a visual task, the monkey's head must be held in a stationary position during recording. Stability is accomplished by cementing a small stainless-steel triangular peg to the frontal bone of the skull under general anesthesia. The monkey is then trained to position the peg in a V-shaped receptable equipped with a microswitch. When the switch is activated, the computer then begins to present visual stimulation for the monkey to discriminate and thus gain fruit juice rewards. The monkey's head is fixed by securing the peg once it is placed into the V-shaped receptacle.

V. THE STUDY OF PERCEPTUAL MEMORY IN BEHAVING OWL MONKEYS

In our laboratory, owl monkeys are being used to explore the mechanisms of perceptual memory. Viewed from an ecological perspective, the main task of the visual cortex is to extract behaviorally meaningful patterns from noisy and ambiguous images of the natural world. Because of the inherent ambiguity of natural images, multiple and conflicting interpretations may be possible. The task of the visual cortex is to select the most appropriate interpretation quickly and reliably. This task must often be performed on the basis of incomplete information. This function requires

a kind of perceptual learning that, we hypothesize, takes place in the visual cortex.

We are exploring this putative learning function of visual cortex through the use of cognitively defined contours, which are the borders of patterns embedded in a noisy background (Fig. 21). These patterns are difficult to see until revealed by special cues such as the brief movement of the pattern with respect to the background. Our perceptual experience with these cognitive contours is that, once they have been revealed, they are very readily seen again and that this capacity persists for months or years for a particular stimulus array. This perceptual learning is reminiscent of a type of long-term learning described by Warrington and Weiskrantz (1968) in amnesic patients. These patients, who had severe deficits in their capacity to remember recent events, showed a remarkable ability to identify visual patterns when they viewed fragmented residues of whole patterns. The amnesic patient, HM, whose medial temporal lobe including hippocampus had been surgically removed bilaterally, showed retention of his capacity to identify fragmented images in these tests (Milner *et al.*, 1968). This capacity has been termed "priming" and has been postulated to be performed by a "perceptual representation system" thought to reside in extrastriate visual cortex (Tulving and Schacter, 1990). Retention due to priming is long-lasting with no decay after 1 week (McAndrews *et al.*, 1987; Musen and Treisman, 1990), and some retention after 3 months (Warrington and Weiskrantz, 1968).

Position emission tomography studies have revealed that priming with visual images produces reduced blood flow upon retesting in a region of

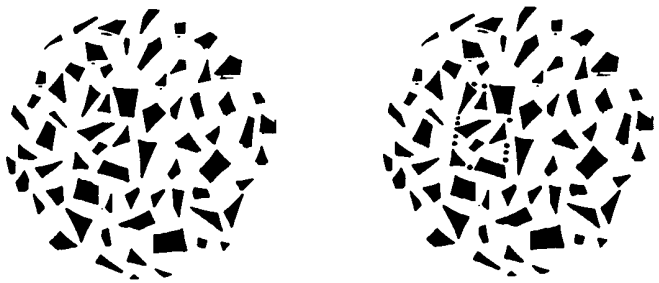

FIGURE 21 Sample stimulus pattern to test visual perceptual memory. A rectangular figure is embedded in the random polygon array. The right figure is not obvious until it is cued (by closure in this example), shown on the right. The subject's task is to report the orientation of the embedded figure before, during, and after cuing. The stimulus was generated by cutting up small slips of black paper and sprinkling them on a white background. The image was then captured as a computer bit map, using a CCD camera with a frame grabber. We can generate an unlimited number of novel stimuli with this simple method. From Jeo and Allman, unpublished stimulus pattern.

right occipital extrastriate visual cortex in human subjects (Squire *et al.*, 1991). This result suggests that priming facilitates the neural solution to perceiving images with consequently less energy expended and presumably a higher signal-to-noise ratio in the neural populations involved. Access to priming memory is hyperspecific in that it depends among other things on the exact geometrical configuration of the priming stimulus (Tulving and Schacter, 1990). Hyperspecificity of access suggests that priming memory may be stored within the visuotopically mapped cortical visual areas.

These experiments can be regarded as a further exploration of the nonclassical responses of visual cortical neurons described earlier in this chapter. These results have been extended to "illusory contours" that were implied by stimuli that were entirely beyond the classical receptive field for neurons in the second visual area (Peterhans and von der Heydt, 1989).

The functional properties of visual cortical neurons have been viewed as very highly specialized filters set to detect different aspects of visual stimuli such as the direction of motion, binocular disparity, orientation, or color. We suggest that in addition to these classical features of visual cortical neurons, there is the capacity to respond selectively to patterns on the basis of prior experience. In other words, visual cortex can "learn to see" ambiguous patterns embedded in a noisy background.

We further suggest that these perceptual learning capacities may be localized in a manner analogous to the evident perceptual specializations present in the various areas. For example, perceptual learning related to differential motion might be preferentially related to area MT. To test this idea we can use different types of cues (differential motion, closure, shading, and stereoscopic depth) to determine whether the nature of the cue might affect the site of storage within the visual cortical areas.

We use stimuli with embedded rectangles that are either horizontal or vertical. The monkeys are trained in an apparatus with two paddle keys and respond to horizontal stimuli by pressing the right key and to vertical stimuli by pressing the left key. The monkeys are then tested to determine whether they respond correctly to the orientation of a series of embedded figures before and after cuing; response time is also measured. Owl monkeys are easily trained to perform visual discrimination tasks and are very good psychophysical subjects. In a typical experiment, a series of different embedded figures are presented in pseudorandom order. Initially, we display each stimulus array without any cues for the embedded figure. We allow the subject to respond to the novel stimulus, then immediately activate the cue for the imbedded rectangle, and the subject is allowed to respond again. After several such presentations, the stimuli is presented without any cues.

To ensure that the subjects are performing the figure detection and not simply memorizing the entire figure, we plan to perform two control experiments. The first will be to measure response to a random polygon

array without any embedded figures, where only one orientation response will be reinforced. The second control experiment will be to compare the effects of rotating elements in the surround with rotating elements forming the contour boundary in the embedded figure. If the subject is responding to the embedded figure and not simply memorizing the entire array, disturbing elements within the embedded figure should disrupt performance more than disturbing surround elements.

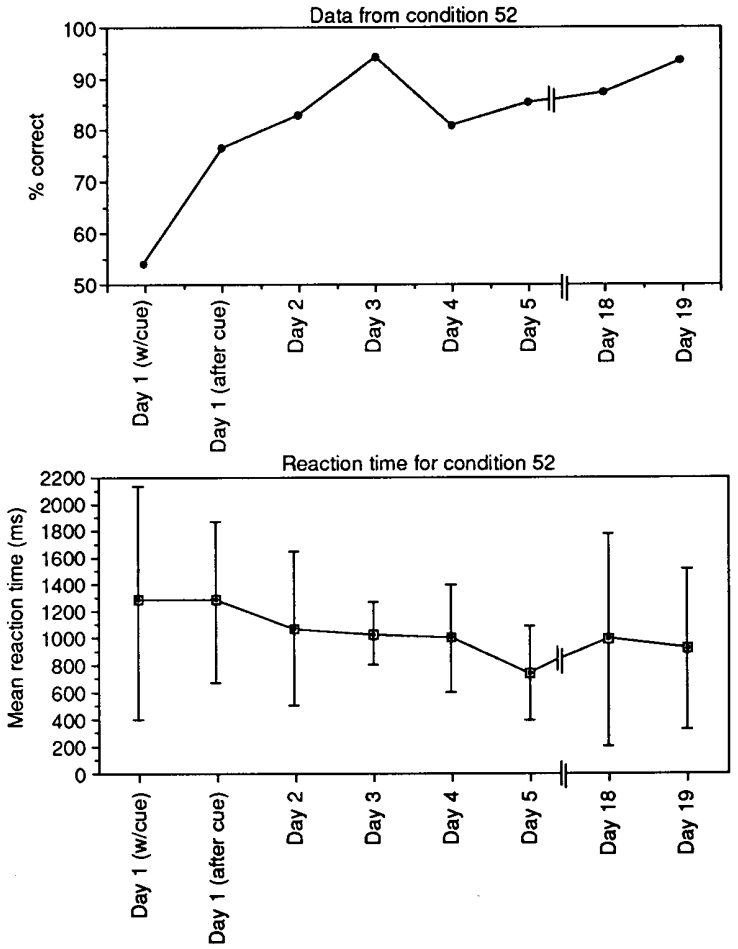

FIGURE 22 Typical owl monkey performance for a new stimulus pattern. Top: Performance goes from chance levels (54%, day 1 without cue) to 76% (Day 1 after cue) and stays at steady levels even after a 13-day break (Day 5–Day 18). Bottom: Reaction time improves slightly from Day 1 to Day 5 and remains constant after a 13-day break. Standard deviation of reaction time decreases from Day 1 to Day 5, but increases after the break. From Jeo and Allman, unpublished data.

We have trained two owl monkeys to perform the perceptual memory task. The monkeys report the orientation of the embedded horizontal or vertical rectangle in a random array of polygons, described earlier. Initially, we displayed stimulus array without any cues for the embedded figure. We allowed the monkey to respond to the novel stimuli and rewarded for a correct answer, then immediately activated the cue for the embedded rectangle, and the monkey was allowed to respond again. After several such presentations, the stimuli were presented without any cues.

Both owl monkeys performed this task very well; one monkey learned over 100 different stimulus patterns. The principle results are: performance is not rotation invariant, that is, when we rotate the entire stimulus 90 degrees, accuracy degrades to chance levels; displaying the stimuli as a mirror image similarly degrades performance; however, performance is contrast sign invariant, such that displaying the images in reverse contrast does not affect accuracy.

The monkeys work daily, can perform up to 1500 trials per day, and will work steadily for 2 to 3 hr. The time that it takes for the monkey to learn a new stimulus varies from one cued presentation for easy figures to many exposures over several training sessions for more difficult ones. Reaction time and its standard deviation both decrease as the stimuli are learned. This knowledge is retained even after several weeks without exposure to the same stimuli (Fig. 22).

REFERENCES

Allman, J., and Kaas, J. (1971a). A representation of the visual field in the caudal third of the middle temporal gyrus in the owl monkey (*Aotus trivirgatus*). *Brain Res.* **31,** 85–105.

Allman, J., and Kaas, J. (1971b). Representation of the visual field in striate and adjoining cortex of the owl monkey (*Aotus trivirgatus*). *Brain Res.* **35,** 89–106.

Allman, J., and Kaas, J. (1974a). The organization of the second visual area (VII) in the owl monkey: A second order transformation of the visual hemifield. *Brain Res.* **76,** 247–265.

Allman, J., and Kaas, J. (1974b). A crescent-shaped area surrounding the middle temporal area (MT) in the owl monkey (*Aotus trivirgatus*). *Brain Res.* **81,** 199–213.

Allman, J., and Kaas, J. (1975). The dorsomedial cortical visual area: A third tie in the occipital lobe of the owl monkey (*Aotus trivirgatus*). *Brain Res.* **100,** 473–487.

Allman, J., and Kaas, J. (1976). Representation of the visual field on the media wall of occipital–parietal cortex in the owl monkey. *Science* **191,** 572–575.

Allman, J., Miezin, F., and McGuinness, E. (1985). Stimulus specific response from beyond the classical receptive field: Neurophysiological mechanisms for local–global comparisons in visual neurons. *Annu. Rev. Neurosci.* **8,** 407–430.

Allman, J., Miezin, F., and McGuinness, E. (1990). The effects of background motion on the responses of neurons in the first and second visual areas (V-I and V-II). In "Local and Global Order in Perceptual Maps" (G. M. Edelman, W. E. Gall, W. M. Cowan, eds.), pp. 131–142, Wiley-Liss, New York.

Allman, J., and Zucker, S. (1991). Cytochrome oxidase and functional coding in primate striate cortex: A hypothesis. *Cold Spring Harbor Symposia on Quantitative Biology* **55,** 979–982.

Baker, J. F., Petersen, S. E., Newsome, W. T., and Allman, J. M. (1981). Visual response properties of neurons in four extrastriate visual areas of the owl monkey (*Aotus trivirgatus*):

A quantitative comparison of medial, dorsomedial, dorsolateral and middle temporal areas. *J. Neurophysiol.* **45,** 397–416.

Born, R. T., and Tootell, R. B. H. (1992). Segregation of global vs. local processin in primate area MT. *Nature (London)* **357,** 497–499.

Horton, J. (1984). Cytochrome oxidase patches: A new cytoarchitectronic feature of monkey cortex. *Philos. Trans. R. Soc. London, B Ser.* **304,** 199–253.

Livingstone, M., and Hubel, D. (1984). Anatomy and physiology of a color system in primate visual cortex. *J. Neurosci.* **4,** 309–356.

McAndrews, M., Glisky, E., and Schacter, D. (1987). When priming persists: Long-lasting implicit memory for a single episode in amnesic patients. *Neuropsychologia* **25,** 497–506.

Milner, B., Corkin, S., and Teuber, H.-L. (1968). Further analysis of the hippocampal amnesic syndrome: A 14-year follow-up study of H.M. *Neuropsychologia* **6,** 215–234.

Musen, G., and Treisman, A. (1990). Implicit and explicit memory for visual patterns. *J. Exp. Psychol.: Learning Memory, Cognition* **16,** 127–137.

Nakayama, K., and Loomis, J. (1974). Optical velocity patterns, velocity-sensitive neurons, and space perception: A hypothesis. *Perception* **3,** 63–80.

Newsome, W. T., and Allman, J. M. (1980). The interhemispheric connections of visual cortex in the owl monkey. *Aotus trivirgatus,* and the bushbaby, *Galago senegalensis. J. Comp. Neurol.* **19,** 209–233.

Peterhans, E., and von der Heydt, R. (1989). Mechanisms of contour perception in monkey visual cortex. I. Contours bridging gaps. *J. Neurosci.* **9,** 1749–1763.

Petersen, S. E., Baker, J. F., and Allman, J. M. (1980). Dimensional selectivity of neurons in the dorsolateral visual area of the owl monkey. *Brain Res.* **197,** 507–511.

Petersen, S. E., Baker, J. F., and Allman, J. M. (1985). Direction-specific adaptation in area MT of the owl monkey. *Brain Res.* **346,** 146–150.

Petersen, S. E., Miezin, F. M., and Allman, J. M. (1988). Transient and sustained responses in four extrastriate visual areas of the owl monkey. *Exp. Brain Res.* **70,** 55–60.

Poggio, G. F., and Fischer, B. (1977). Binocular interactions and depth sensitivity in striate and prestriate cortex of behaving rhesus monkeys. *J. Neurophysiol.* **40,** 1392–1405.

Sereno, M., and Allman, J. (1991). Cortical visual areas in mammals. In "The Neural Basis of Visual Function" (A. Levinthal, ed.), pp. 160–172. Macmillan, London.

Sereno, M., MacDonald, C., and Allman, J. (1987). Multiple visual areas between V2 and MT in the owl monkey. *Soc. Neurosci. Abstr.* **13,** 625.

Squire, L., Ojemann, J. Miezin, F., Petersen, S., Videen, T., and Raichle, M. (1991). Activation of the hippocampus in normal humans: A functional anatomical study of human memory. *Proc. Natl. Acad. Sci. U.S.A.* **89,** 1837–1841.

Tootell, R. B. H., Hamilton, S. L., and Silverman, M. S. (1985). Topography of cytochrome oxidase activity in owl monkey cortex. *J. Neurosci.* **5,** 2786–2800.

Tootell, R. B. H., Silverman, M., Hamilton, S., DeValois, R., and Switkes, E. (1988). Functional anatomy of macaque striate cortex. III. Color. *J. Neurosci.* **8,** 1569–1593.

T'so D., and Gilbert, C. (1988). The organization of chromatic and spatial interactions in primate striate cortex. *J. Neurosci.* **8,** 1712–1727.

Tulving, E., and Schacter, D. (1990). Priming and human memory systems. *Science* **247,** 301–306.

Warrington, E., and Weiskrantz, L. (1968). New method of testing long-term retention with special reference to amnesic patients. *Nature (London)* **217,** 972–974.

Weller, R., and Kaas, J. (1985). Cortical projections of the dorsolateral visual area in owl monkeys: The prestriate relay to inferior temporal cortex. *J. Comp. Neurol.* **234,** 35–59.

Weller, R., and Kaas, J. (1987). Subdivisions and connections of inferior temporal cortex in owl monkeys. *J. Comp. Neurol.* **256,** 137–172.

Wong-Riley, M., and Carroll, E. (1984). The effect of impulse blockage on cytochrome oxidase activity in the monkey visual system. *Nature (London)* **307,** 262–264.